nature photonics

FOCUS | REVIEW ARTICLES

PUBLISHED ONLINE: 18 SEPTEMBER 2011 | DOI: 10.1038/NPHOTON.2011.206

Optofluidic microsystems for chemical and biological analysis

Xudong Fan[1] and Ian M. White[2]

Optofluidics — the synergistic integration of photonics and microfluidics — is a new analytical field that provides a number of unique characteristics for enhancing the sensing performance and simplifying the design of microsystems. This Review describes various optofluidic architectures developed over the past five years, emphasizes the mechanisms by which optofluidics enhances biological/chemical analytic capabilities, including sensing and the precise control of biological micro- and nanoparticles, and also highlights new research directions to which the field of optofluidics may lead.

Optics has long been used to analyse biological and chemical samples. In recent decades, optical sensing systems have evolved from bulk systems, such as flow cytometers and microplate readers, to microdevices, such as on-chip waveguides and resonators. This period has also seen the emergence of microfluidics, which enables small-volume sample handling for performing automated functions such as particle sorting and separation, cell culturing and concentration gradient formation. Recent technological advances in the fields of photonics and microfluidics have led to the development of optofluidics, in which photonic and microfluidic architectures are integrated to synergistically provide enhanced function and performance.

Optofluidics has found a broad range of applications since its debut a few years ago, as described in accompanying Reviews by Erickson *et al.*[1] and Schmidt and Hawkins[2] in this Focus Issue, as well as in other recent publications[3–6]. In particular, optofluidics is well-suited for biological/chemical detection and analysis in extremely small detection volumes (femtolitres to nanolitres) because it integrates sample preparation and delivery with the analytical mechanism. As illustrated by many of the examples presented in this Review, microfluidics is not merely an add-on accessory to an optofluidic device, but rather comprises an integral part of it[7–10]. Such integration provides a number of unique characteristics that can be leveraged for biological/chemical analysis. Many optical properties, such as refractive index (RI), fluorescence, Raman scattering, absorption and polarization, can be exploited individually or in combination to generate the sensing signal. Detection can be carried out in either the linear[7–10] or nonlinear optical regime[11–13]. Adaptation of traditional analytical chemistry technologies such as chromatography and electrophoresis to optofluidic devices further increases their functionality in biological/chemical analysis[14–18]. Furthermore, optofluidic microsystems can also employ optical forces in tandem with microfluidics to trap and manipulate targets, thus further enhancing the system's analytical capabilities[19].

This Review summarizes state-of-the-art optofluidic architectures in biological/chemical analysis. The analytical mechanisms are grouped into four sections: RI detection, fluorescence detection, surface-enhanced Raman spectroscopy (SERS) detection, and optical trapping and manipulation. The use of optofluidics to enhance overall analytical performance is emphasized and the potential future advances of optofluidics in biological/chemical analysis are discussed.

Optofluidic sensors with RI-based detection

Measuring the RI of a sample is one of the most popular biological/chemical analysis methods used in optofluidic sensors. This technique is primarily distinguished as being label-free, in contrast with fluorescence labelling. Optofluidic RI sensors measure RI changes of a bulk solution due to the homogeneous presence of analytes, as these typically have a different RI (or excess polarizability) from that of the background solution. RI detection is particularly attractive for optofluidic sensors that have extremely small detection volumes because the RI signal scales with the analyte bulk concentration or surface density, rather than with the total number of molecules. In many optofluidic RI sensors, the electric field can be confined to a small volume (femtolitres to nanolitres), thus enabling ultralow quantities of molecules to be detected. Various optofluidic architectures, including metallic nanohole-array-based plasmonics[8,20–24] (Fig. 1a), photonic crystals and photonic crystal fibres (PCFs)[9,25–34] (Fig. 1b,c), as well as interferometric structures such as ring resonators[35–40] (Fig. 1d,e), Mach–Zehnder interferometers[41,42] and Fabry–Pérot cavities[10,43–45] (Fig. 1f) have been explored as ways of maximizing the light–analyte interaction while satisfying other requirements in biological/chemical analysis.

Optofluidic RI sensors based on plasmonics, photonic crystals or PCFs are primarily composed of periodic metallic or dielectric structures that can be used to confine and guide light (Fig. 1a–c). The voids in these structures are inherently excellent microfluidic channels to fill with liquid samples for biological/chemical sensing. A surface detection sensitivity of the order of 1 nm nm^{-1} (that is, a spectral shift of 1 nm for every nanometre of molecular attachment, where a 1 nm increase in height at the sensor surface corresponds to a biomolecular attachment of approximately 1 ng mm^{-2})[46,47] has been demonstrated[20,27,30]. The extremely small effective sensing area in such schemes allows subfemtogram biomolecules to be detected[27,29]. Unfortunately, in practice, such unprecedented detection capability is usually plagued by the rudimentary sample delivery system, which is often unable to deliver analytes selectively to where the light–matter interaction is strongest.

Researchers have recently reported optofluidic techniques that integrate the photonic device with a microfluidic channel for simple and repeatable sample delivery. The optofluidic ring resonator (OFRR) is an example of such an optofluidic advancement[35–40] (Fig. 1d,e). OFRRs have been realized using thin-walled cylindrical capillaries, on-chip self-assembled tubes, glass microbubbles and antiresonant reflecting optical waveguides (ARROWs). OFRRs

[1]Biomedical Engineering Department, University of Michigan, Ann Arbor, Michigan 48109, USA. [2]Fischell Department of Bioengineering, University of Maryland, College Park, Maryland 20742, USA. e-mail: xsfan@umich.edu; ianwhite@umd.edu

NATURE PHOTONICS DOI: 10.1038/NPHOTON.2011.206

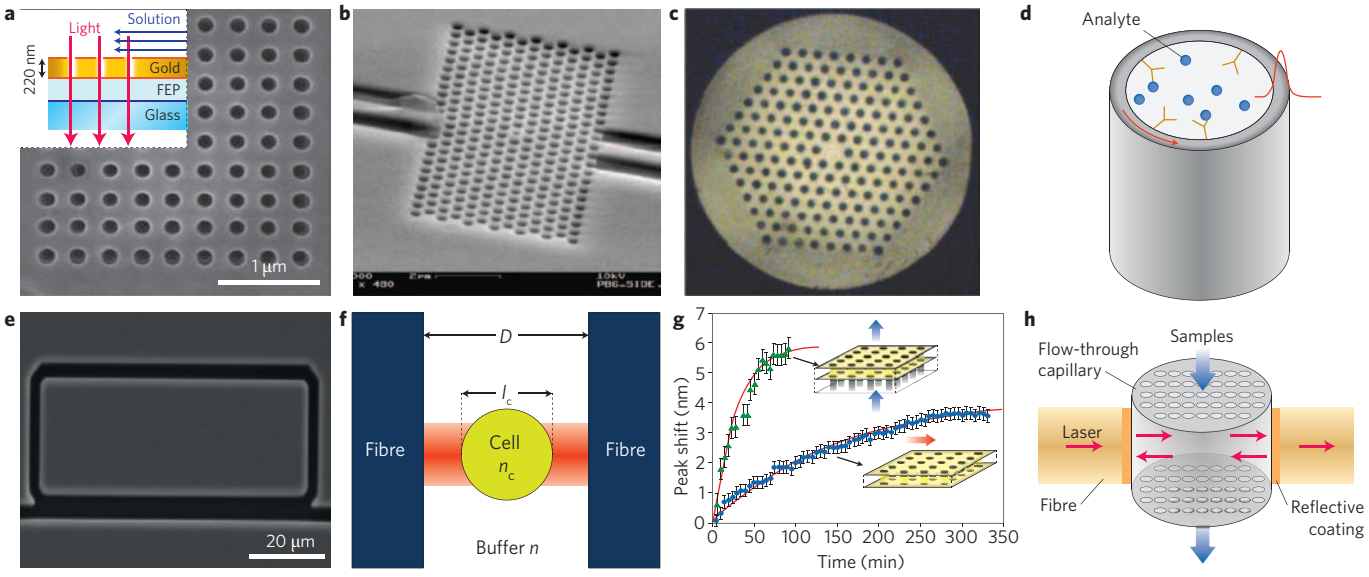

Figure 1 | Various optofluidic devices used in RI detection. a, Metallic nanohole-array-based plasmonic sensor[21]. **b**, Dielectric planar photonic crystal sensor[27]. **c**, PCF-based sensor[30]. **d**, Capillary-based OFRR sensor. **e**, ARROW-based OFRR[40]. **f**, Fabry–Pérot interferometric sensor for cell detection[42]. **g**, Flow-through and flow-over plasmonic sensors, together with each system's sensing response[8]. **h**, Fabry–Pérot sensor with flow-through micro- and nanofluidic channels[10]. Figure reproduced with permission from: **a**, ref. 21 © 2008 ACS; **b**, ref. 27 © 2007 OSA; **c**, ref. 30 © 2006 OSA; **e**, ref. 40 © 2010 AIP; **f**, ref. 42 © 2007 AIP; **g**, ref. 8 © 2009 ACS; **h**, ref. 10 © 2011 AIP.

retain the excellent sensing capability of ring resonators[48] while also being integrated microfluidic structures. Researchers have used OFRRs to detect various chemical and biological samples, ranging from small molecules such as biotin to large species such as viral particles[38,49]. The achievable detection sensitivity of such schemes is around 570 nm per RIU (refractive index unit) for bulk RI detection and 0.02 nm nm^{-1} for surface detection, with detection limits of 10^{-7} RIU and 1 pg mm^{-2}, respectively[38]. An optofluidic Fabry–Pérot cavity sensor is similar to an OFRR in that the liquid channel is part of the sensing cavity[43–45]. Fabry–Pérot sensors probe the entire sample volume to enable 'whole body' detection, which is particularly useful for cell detection (Fig. 1f). Using this method, Shao *et al.* differentiated lymphoma cells from normal lymphocytes[44].

Another problem faced by photonic sensors, even when integrated with a microfluidic sample delivery system, is transporting a large number of target molecules to the sensor surface. Very recently, researchers replaced the 'flow-over' technique with an optofluidic 'flow-through' strategy to mitigate the slow mass-transport issues experienced by most optical sensors. This optofluidic technique integrates nanofluidic channels through the optical sensing structure such that the entire sample interacts directly with the sensing surface. Mass transport to the sensing surface is almost entirely convective (instead of diffusive), which provides a stronger signal in significantly less time than the conventional flow-over sensor. Plasmonic nanofluidic sensors and photonic crystal nanofluidic sensors fabricated by photolithography consist of arrays of nanoholes, as shown in Fig. 1g[8,9,23,24]. The wafer substrate is back-etched so that the liquid can be driven through the thin (~100 nm) holey metal or dielectric membrane. Researchers have achieved bulk RI sensitivity and surface attachment sensitivities of 600 RIU nm^{-1} and 2 nm nm^{-1}, respectively[8,23], as well as 14-fold and 6-fold enhancements in the mass-transport rate over the established flow-over method for bulk solution and small molecules, respectively[8,23] (Fig. 1g). Guo *et al.* developed an alternative flow-through design, which is illustrated in Fig. 1h[10]. Thousands of submicrometre-sized holes in a capillary form both nanofluidic channels and part of a Fabry–Pérot cavity. This optonanofluidic sensor is similar to the nanoporous sensor[50,51] except that it has well-defined flow-through holes fabricated using the drawing method. Therefore, it exhibits a high surface mass sensitivity (10–20 nm nm^{-1}) resulting from the large surface-to-volume ratio, while achieving much more efficient sample delivery than the traditional nanoporous sensor.

Researchers have also enhanced sample analysis capabilities by incorporating optofluidic RI sensors into traditional analytical chemistry technologies such as chromatography and electrophoresis. This marriage often allows the resulting device to function as a separation column and on-column detector, which allows the separated analytes to be detected in real-time and minimizes microfluidic connections. Wang *et al.* and Zhu *et al.* developed examples of on-column optofluidic RI sensors using back-scattering interferometry[14] and thin-walled capillary OFRRs[15] — both of which measure the bulk RI change at any predetermined location along the column when analytes pass through the detection zone.

Fluorescence-based optofluidic sensors

Although label-free sensing is advantageous in many situations thanks to its low number of biosensing steps, many applications benefit from fluorescence-based sensing. One of the major research directions in optofluidic fluorescence detection is to improve the confinement and guiding of light in low-RI analyte-containing buffer solutions, which enhances the light–fluorophore interaction and fluorescence collection efficiency and thus boosts the detection limit. Various optofluidic architectures have been developed to achieve this goal: liquid-core waveguides using low-index cladding materials such as Teflon[52,53] and nanoporous materials[54,55] to guide the light through total internal reflection; photonic crystal structures that enhance the fluorescence signal and thus provide better fluorescence collection efficiency[56–60]; and slot waveguides that confine both liquid and light within the same submicrometre-sized channel[61]. Among these, the ARROW is one of the most promising optofluidic sensing structures for confining and guiding both light and liquid[7,40,62–66]. Used in fluorescence detection[7,62,63,66], the ARROW is able to achieve a subpicolitre excitation or detection volume, thus enabling sensitive detection even at extremely low

analyte quantities. Schmidt, Hawkins and co-workers demonstrated the detection of a single molecule and a single particle in free solution, both directly and through fluorescence correlation spectroscopy[7,62,66]. The same team recently used dual-colour fluorescence cross-correlation spectroscopy to detect particle co-localization and, when combined with fluorescence resonance energy transfer (FRET), DNA binding and denaturation[63]. These achievements may allow rapid and *in situ* biological/chemical analysis by replacing conventional bulky and expensive fluorescence microscopes with inexpensive optofluidic devices.

The optofluidic laser is another versatile and promising platform for biological/chemical analysis. Such devices usually consist of a microfluidic laser cavity to provide optical feedback and a fluorophore solution as the gain medium, which enables intracavity detection. In contrast with other optofluidic fluorescence sensors discussed above, the optofluidic laser sensor relies on stimulated emission as the sensing signal and is therefore highly sensitive to small perturbations in the laser cavity or gain medium. Several recent intracavity sensing demonstrations have particularly revealed the vast capabilities of the optofluidic laser. Using a simple optofluidic dye laser based on a Fabry–Pérot cavity, Galas *et al.* carried out sensitive intracavity absorption measurements based on the change in laser emission intensity[11]. More recently, Sun *et al.* used an OFRR laser in conjunction with FRET to achieve sensitive DNA detection[12]. The hybridization of the DNA probe and target causes FRET between the donor and acceptor, leading to a drastic reduction in the initial lasing emission from the donor and the simultaneous emergence of lasing from the acceptor, which significantly increases the sensing signal above that of conventional FRET. The same group recently reported the highly selective detection of single-nucleotide polymorphisms using the OFRR and molecular beacon approach[13]. In the presence of the target DNA, the OFRR is operated above the lasing threshold, which generates strong laser emission. In contrast, with single-base mismatched DNA, the OFRR is below the lasing threshold and thus only a negligible fluorescence background is observed. Through this 'analog-to-digital' detection scheme, enhancements of over two orders of magnitude in the discrimination ratio between the target and single-base mismatched DNA have been achieved.

Optofluidic SERS-based analysis

SERS has the potential to combine the simplicity of label-free analysis, the low detection limits of fluorescence-based detection and the molecular-specific Raman spectrum for analyte identification. SERS utilizes the well-understood electromagnetic enhancement provided by metal nanostructures[68] as well as a chemical enhancement resulting from metal–molecule interactions, which is not yet well understood[69,70], to increase the Raman scattering cross-section by several orders of magnitude. SERS has even been used to observe Raman scattering from single molecules[71,72]. Although it has been nearly 35 years since the first demonstrations of SERS[73,74], the practical applications of this powerful technique are still quite limited.

One way of improving the practical application of SERS is to integrate the detection mechanism into a microfluidic system that boasts other functions. Two common implementations are to pass the sample through a channel in a metal nanoparticle colloid solution, and to integrate a metal nanostructured surface at the bottom of a microfluidic channel. In general, however, conducting SERS measurements within a microfluidic environment can be detrimental to the detection limit because of the reduced number of SERS-active sites when integrating with a metal nanostructured surface and the low mass-transport of analyte molecules to the SERS-active surface in a microfluidic environment. Recent optofluidic SERS approaches compensate for these shortcomings by increasing the number of target analyte molecules that are excited by the excitation source or that interact with SERS-active surfaces, which, as a result, improves the SERS performance.

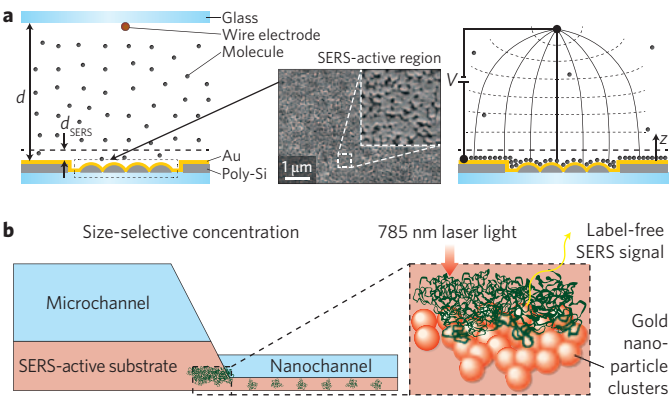

Figure 2 | Optofluidic SERS techniques. a, Electrokinetic concentration of analyte molecules at the SERS-active surface in a microchannel[82]. **b**, Size-selective detection of protein aggregates using a nanofluidic channel[85]. Figure reproduced with permission from: **a**, ref. 82 © 2009 RSC; **b**, ref. 85 © 2011 RSC.

One optofluidic method of improving the performance of a SERS set-up is to utilize photonic geometries that extend the detection volume, thus including a higher number of analyte molecules and SERS-active sites. For example, PCFs (Fig. 1c) utilize a holey core or cladding as a microfluidic channel; the excitation light and Raman-scattered photons propagate along with the sample inside the PCF and thus the detection volume extends for the entire length of the PCF. Yang *et al.* used the hollow core of a PCF as a microfluidic channel[75], whereas Khaing Oo *et al.* utilized a holey cladding[76]. In both cases, the reported detection limit for rhodamine 6G (R6G) was around 100 pM, which is significantly larger than the reported detection limits of the conventional microfluidic SERS approaches described above. This optofluidic SERS concept was translated to an on-chip implementation by Measor *et al.*[77] using the ARROW structure discussed previously, which combines the optofluidic SERS enhancement with the ability to integrate other on-chip functions with SERS detection.

SERS can also be improved by using micro- and nanofluidic techniques to concentrate analytes or analyte–nanoparticle aggregates in the detection volume. This increases the performance and utility of SERS by eliminating the reliance on diffusion for carrying targets to the detection volume. Wang *et al.* showed that this can be achieved passively by using nanoscale geometries that concentrate the aggregates, and in particular through a device that utilizes a 40-nm-high channel between the inlet and outlet[78]. In this scheme, metal nanoparticles were trapped at the inlet of the nanochannel, which resulted in a high density of SERS-active sites. Through a similar concept, Park *et al.* detected a Cy3-labelled DNA sequence marker for the dengue virus[79]. In this case, the authors formed nanofluidic channels as small as 60 nm using elastomeric collapse in polydimethylsiloxane (PDMS) at the inlet. Liu *et al.* utilized a nanoporous polymer monolith within a microfluidic channel to trap and concentrate silver nanoparticles in a three-dimensional (3D) matrix[80]. This design created a 3D SERS-active matrix, thus eliminating the need for analyte molecules to diffuse to the surface.

Active microfluidic techniques have also been used in optofluidic SERS techniques to concentrate the nanoparticles or analyte molecules (or both) prior to SERS detection. Huh *et al.* concentrated nanoparticle–target conjugates in the SERS detection volume by using electrokinetic forces to attract metal nanoparticles within the microfluidic chamber[81]. Electrokinetic forces can also be used to

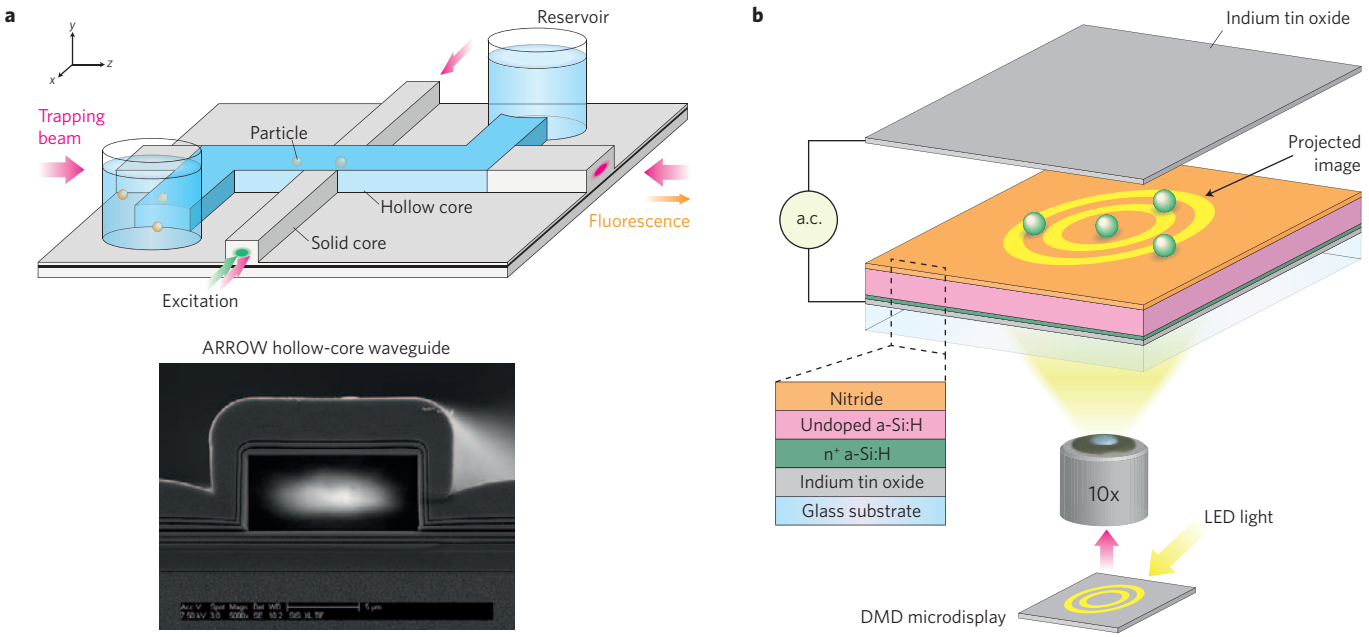

Figure 3 | Optofluidic devices for nanoparticle trapping and manipulation. a, Particle trapping and fluorescence analysis using a liquid-core ARROW waveguide structure[65]. **b**, Optoelectronic tweezers for the parallel control of cells in a microfluidic channel[94]. Figure reproduced with permission from: **a**, ref. 65 © 2009 RSC; **b**, ref. 94 © 2005 NPG.

concentrate the analyte at a SERS-active surface. Cho *et al.* created a microfluidic channel on top of a SERS-active surface and fabricated an electrode on the top of the channel[82]. Applying a potential between the electrode and the metal-nanostructured surface drove the analyte molecules to the SERS-active surface, thus concentrating all of the analyte in the sample volume to the detection zone (Fig. 2a) and again avoiding the need to rely on diffusion for interaction between the SERS-active surfaces and the analyte. Exploiting the tremendous enhancement offered by this microfluidic technique, Cho *et al.* detected adenine at a concentration of 10 fM.

Another optofluidic approach that holds great potential for increasing the performance of SERS is using optofluidic resonators for SERS excitation within a micro- or nanofluidic environment. The high-intensity field at the surface of an optical resonator can function as a high-power excitation source for SERS. Although there are a few reports of using optical resonators as sources of SERS excitation[83,84], this optofluidic design concept remains mostly unexplored. Furthermore, building on some of the developments in optofluidics, there is great potential to integrate the optofluidic resonator approach with the micro- or nanofluidic concentration approaches outlined above, which could together provide extraordinary SERS performance.

Aside from increasing detection capabilities, optofluidics also allows for unique applications of SERS that have not been possible until now. For example, building on the PDMS nanochannels described above, Choi *et al.* have reported the selective detection of protein aggregates, which play a role in the detection of a number of diseases, including Alzheimer's[85]. After nanoparticles form a concentrated network at the inlet of the nanochannel, aggregated proteins are trapped in the detection zone and thus produce a SERS signal, while monomer proteins migrate through the detection zone and are not detected (Fig. 2b). Another application of optofluidic SERS recently demonstrated by Lee *et al.* is to incorporate an on-column SERS-based detector with the chromatographic separation of metal ions[18]. The inside surface of the capillary, which is coated with carboxylated gold nanoparticles, serves not only as the separation medium due to the selective adsorption properties of the metal ions, but also as the SERS-active surface. This eliminates the need for a post-separation detection mechanism such as mass spectrometry. It is expected that applications of SERS will continue to emerge from other new advancements in optofluidics, including the introduction of optically resonant microfluidic structures, SERS integration with droplet microfluidics[86] and the optical trapping of nanosized particles.

Optofluidic particle trapping and manipulation

Optical trapping and the precise control of biological micro- and nanoparticles in microfluidics improves the analytical capabilities of microsystems because the particles can be delivered to and held at the sensing/imaging locations, rather than relying on brief, transient interactions. For example, forces in microfluidic channels can be used to hold cells in place for imaging[87] or to focus biomolecules at the sensing region to improve the detection limit[81,82,88]. In addition, plasmon-based trapping allows trapped particles to be analysed using plasmonic sensors[89]. The combination of optofluidic techniques with optofluidic sensing has led to inherently integrated methods for the analysis of biological micro- and nanoparticles in microsystems. Many of the recently reported optofluidic particle manipulation techniques and the physical mechanisms involved are described in an accompanying Review by Schmidt and Hawkins[2], as well as in a recent comprehensive review[19]. Described below are several uses of optofluidic micro- and nanoparticle manipulation that have been demonstrated for biological applications.

The ARROW liquid-core waveguide device was highlighted above for its unique optofluidic ability to allow light to propagate along a microfluidic channel with the sample. Kühn *et al.* recently used the ARROW structure as a low-power optofluidic trap for small particles, including *Escherichia coli* bacteria[65]. As shown in Fig. 3a, light is coupled into each end of an optofluidic waveguide; the optical power gradient resulting from the waveguide loss causes the trapping forces to be directed towards the longitudinal centre of the channel. In addition, solid waveguides are located perpendicular and adjacent to the ARROW to allow fluorescence spectroscopic analysis on trapped particles. In a later design, the authors reduced the optical power

necessary for trapping to approximately 1 μW, which is dramatically lower than that of typical optical tweezer systems[66]. One could also envision a number of interesting applications for an integrated optofluidic trapping and analysis device, such as for monitoring the integrity of a particular pathogenic bacterium while antibiotics are passed through the channel, or for dynamically recording the binding of ligands to the receptors of a trapped biological particle.

An alternative way of creating the high-intensity optical power gradients needed to trap particles in a microfluidic environment is to leverage the properties of optical resonators. Earlier in this Review, we described how 1D photonic crystal resonators can be coupled to waveguides for RI sensing. Light at a particular frequency forms a standing wave in the resonator, with a high-intensity field at the defect. Mandal *et al.* demonstrated the use of this resonator for trapping particles as small as 48 nm (ref. 90). Similarly, Arnold *et al.* and Lin *et al.* have shown that a whispering gallery mode of an optical ring resonator can trap nanoparticles[91] and move them along the ring resonator[92]. Both of these resonator-based traps can use either RI or fluorescence mechanisms to analyse the trapped particles in real time. Arnold *et al.* demonstrated that the microsphere carousel trap could determine the size of the trapped particle; RI-based signal fluctuations caused by the radial Brownian motion of the nanoparticle reveal the radial trapping potential and thus the nanoparticle size[91].

Optical tweezers have been the typical tool of choice for manipulating large biological particles such as mammalian cells. Although useful combinations of optical tweezers and microfluidics have been demonstrated[87,93], these systems can be cumbersome and often require high optical powers. An alternative has been developed that enables the simultaneous optical control and manipulation of a large number of cells within a microfluidic chip. Chiou *et al.* developed optoelectronic tweezers, which utilize photocurrent-induced dielectrophoresis across a microfluidic environment (Fig. 3b)[94]. The technique involves applying an a.c. voltage across a microfluidic channel sandwiched between an indium tin oxide layer and a photoconductive layer. Illuminating the photoconductive material converts it into a conductive electrode, resulting in dielectrophoretic forces due to electric field gradients within the liquid medium. Projecting an optical image onto the photoconductive layer causes electric field gradients that originate only from the illuminated areas; this provides dielectrophoretic control over the cells in the pattern of the projected image (Fig. 3b). Chiou *et al.* used this approach to create 15,000 parallel traps at an optical power five orders of magnitude lower than that of typical optical tweezers. This technique has the potential to greatly advance the capabilities of optofluidic imaging and analysis by performing complicated steering as well as parallel and selective trapping of cells prior to analysis. One can envision the use of video technology based on micro-electromechanical systems to create dynamic images for the simultaneous trapping, complex manipulation and sorting of multiple cells.

Outlook

Optofluidics represents one of the most significant and active advances in the use of photonics for biological/chemical analysis. Over the next five years, the concept of optofluidics is sure to be accepted by end-users outside the sensing community and a number of optofluidic microsystems and technologies currently under research will undoubtedly be commercialized to solve biochemical and biomedical problems in simpler and more cost-effective ways. To take full advantage of optofluidics, we envision several new directions of research.

Imaging. Optofluidics has been used extensively to develop a high-resolution (submicrometre) and low-cost imaging system that has the potential to replace the traditional bulky and expensive microscope[95,96]. This system usually relies on microfluidics for sample transport, CCD/CMOS chips and masks for imaging, and post-analysis computer algorithms for reconstructing high-resolution images. Such imaging techniques have great potential for cellular analysis in remote or resource-limited locations.

Gas analysis. Optofluidics also has important applications for the detection of gases. One detection architecture involves the use of PCF, which can guide both the gas and light along its length to maximize the light–analyte interaction. Both RI- and absorption-based gas detection with PCF have been demonstrated so far[97,98]. However, RI detection lacks specificity, whereas absorption, although highly specific, requires the laser to cover the wide spectral range of various gas molecules. To address these issues, researchers recently used the OFRR in conjunction with microgas chromatography to achieve rapid and specific gas analysis. The OFRR serves as both a gas chromatography column and an on-column optical gas sensor[16,17], thus minimizing the number of connections and the dead volume in conventional microgas chromatography configurations. The separation and detection of twelve gas analytes in four minutes has been demonstrated[17].

Enhancement of the light–matter interaction while reducing sample volume. Improvements in the fields of photonic and microfluidic engineering now allow the light and sample to be confined to femtolitre volumes, which represents a 100- to 1,000-fold reduction in sample volume over most standard optofluidic devices. Strong interactions in such a small volume may allow the detection of single molecules using label-free or SERS detection without the need for fluorophore labelling.

System integration using optofluidics. The development of optofluidic systems or subsystems (rather than components) by the adaptation and incorporation of technologies such as chromatography[18], electrophoresis[14,15], photophoresis[99] and nanopores[64] into sample separation, purification and pre-concentration stages will significantly enhance current biological/chemical analysis capabilities. In addition, multimodal detection involving combinations of RI, fluorescence and SERS in both the linear and nonlinear regime could be used to provide complementary information in biological/chemical analysis.

Advancing the synergy between particle control and sensing. Although optofluidic particle control and sensing can be applied to detection, we envision that its largest impact will be related to bioprocess discovery at the cellular and molecular level. For example, this technique could replace the large laser tweezer systems used today for studying protein folding energy landscapes and protein binding energies.

In addition, the broad reach of optofluidics may result in unforeseen directions of research. It is clear that research in microfluidics is no longer simply the miniaturization of fluidic components, and that photonics-based analysis has moved beyond the goal of merely achieving smaller biological/chemical sensors. Optofluidics has synergistically linked these two fields, resulting in smart microsystems that enable new applications in biological and chemical analysis.

References

1. Erickson, D., Sinton, D. & Psaltis, D. Optofluidics for energy applications. *Nature Photon.* **5,** 583–590 (2011).
2. Schmidt, H. & Hawkins, A. R. The photonic integration of non-solid media using optofluidics. *Nature Photon.* **5,** 598–604 (2011).
3. Psaltis, D., Quake, S. R. & Yang, C. Developing optofluidic technology through the fusion of microfluidics and optics. *Nature* **442,** 381–386 (2006).
4. Monat, C., Domachuk, P. & Eggleton, B. J. Integrated optofluidics: A new river of light. *Nature Photon.* **1,** 106–114 (2007).

5. Hawkins, A. R. & Schmidt, H. (eds) *Handbook of Optofluidics* (CRC, 2010).
6. Fainman, Y., Lee, L., Psaltis, D. & Yang, C. (eds) *Optofluidics: Fundamentals, Devices, and Applications* (McGraw-Hill, 2010).
7. Yin, D., Deamer, D. W., Schmidt, H., Barber, J. P. & Hawkins, A. R. Single-molecule detection sensitivity using planar integrated optics on a chip. *Opt. Lett.* **31,** 2136–2138 (2006).
8. Eftekhari, F. *et al.* Nanoholes as nanochannels: Flow-through plasmonic sensing. *Anal. Chem.* **81,** 4308–4311 (2009).
9. Huang, M., Yanik, A. A., Chang, T. & Altug, H. Sub-wavelength nanofluidics in photonic crystal sensors. *Opt. Express* **17,** 24224–24233 (2009).
10. Guo, Y. *et al.* Optofluidic Fabry–Pérot cavity biosensor with integrated flow-through micro-/nanochannels. *Appl. Phys. Lett.* **98,** 041104 (2011).
11. Galas, J. C., Peroz, C., Kou, Q. & Chen, Y. Microfluidic dye laser intracavity absorption. *Appl. Phys. Lett.* **89,** 224101 (2006).
12. Sun, Y., Shopova, S. I., Wu, C.S., Arnold, S. & Fan, X. Bioinspired optofluidic FRET lasers via DNA scaffolds. *Proc. Natl Sci. Acad. USA* **107,** 16039–16042 (2010).
13. Sun, Y. & Fan, X. Highly selective single-nucleotide polymorphism detection with optofluidic ring resonator lasers. *CLEO/QELS* paper CWL6 (2011).
14. Wang, Z., Swinney, K. & Bornhop, D. J. Attomole sensitivity for unlabeled proteins and polypeptides with on-chip capillary electrophoresis and universal detection by interferometric backscatter. *Electrophoresis* **24,** 865–873 (2003).
15. Zhu, H., White, I. M., Suter, J. D., Zourob, M. & Fan, X. Integrated refractive index optical ring resonator detector for capillary electrophoresis. *Anal. Chem.* **79,** 930–937 (2007).
16. Shopova, S. I. *et al.* On-column micro gas chromatography detection with capillary-based optical ring resonators. *Anal. Chem.* **80,** 2232–2238 (2008).
17. Sun, Y. *et al.* Rapid tandem-column micro-gas chromatography based on optofluidic ring resonators with multi-point on-column detection. *Analyst* **135,** 165–171 (2010).
18. Lee, S. J. & Moskovits, M. Visualizing chromatographic separation of metal ions on a surface-enhanced Raman active medium. *Nano Lett.* **11,** 145–150 (2011).
19. Erickson, D., Serey, X., Chen, Y.F. & Mandal, S. Nanomanipulation using near field photonics. *Lab Chip* **11,** 995–1009 (2011).
20. Pang, L., Hwang, G. M., Slutsky, B. & Fainman, Y. Spectral sensitivity of two-dimensional nanohole array surface plasmon polariton resonance sensor. *Appl. Phys. Lett.* **91,** 123112 (2007).
21. Yang, J.C., Ji, J., Hogle, J. M. & Larson, D. N. Metallic nanohole arrays on fluoropolymer substrates as small label-free real-time bioprobes. *Nano Lett.* **8,** 2718–2724 (2008).
22. Im, H., Lesuffleur, A., Lindquist, N. C. & Oh, S.H. Plasmonic nanoholes in a multichannel microarray format for parallel kinetic assays and differential sensing. *Anal. Chem.* **81,** 2854–2859 (2009).
23. Yanik, A. A., Huang, M., Artar, A., Chang, T. & Altug, H. Integrated nanoplasmonic-nanofluidic biosensors with targeted delivery of analytes. *Appl. Phys. Lett.* **96,** 021101 (2010).
24. Escobedo, C., Brolo, A. G., Gordon, R. & Sinton, D. Flow-through vs flow-over: Analysis of transport and binding in nanohole array plasmonic biosensors. *Anal. Chem.* **82,** 10015–10020 (2010).
25. Chow, E., Grot, A., Mirkarimi, L. W., Sigalas, M. & Girolami, G. Ultracompact biochemical sensor built with two-dimensional photonic crystal microcavity. *Opt. Lett.* **29,** 1093–1095 (2004).
26. Lee, M. R. & Fauchet, P. M. Nanoscale microcavity sensor for single particle detection. *Opt. Lett.* **32,** 3284–3286 (2007).
27. Lee, M. R. & Fauchet, P. M. Two-dimensional silicon photonic crystal based biosensing platform for protein detection. *Opt. Express* **15,** 4530–4535 (2007).
28. Nunes, P. S., Mortensen, N. A., Kutter, J. P. & Mogensen, K. B. Photonic crystal resonator integrated in a microfluidic system. *Opt. Lett.* **33,** 1623–1625 (2008).
29. Mandal, S., Goddard, J. M. & Erickson, D. A multiplexed optofluidic biomolecular sensor for low mass detection. *Lab Chip* **9,** 2924–2932 (2009).
30. Rindorf, L. *et al.* Photonic crystal fiber long-period gratings for biochemical sensing. *Opt. Express* **14,** 8224–8231 (2006).
31. Huy, M. C. P. *et al.* Three-hole microstructured optical fiber for efficient fiber Bragg grating refractometer. *Opt. Lett.* **32,** 2390–2392 (2007).
32. Rindorf, L. & Bang, O. Highly sensitive refractometer with a photoniccrystalfiber long-period grating. *Opt. Lett.* **33,** 563–565 (2008).
33. He, Z., Zhu, Y. & Du, H. Long-period gratings inscribed in air- and water-filled photonic crystal fiber for refractometric sensing of aqueous solution. *Appl. Phys. Lett.* **92,** 044105 (2008).
34. Wu, D. K. C., Kuhlmey, B. T. & Eggleton, B. J. Ultrasensitive photonic crystal fiber refractive index sensor. *Opt. Lett.* **34,** 322–324 (2009).
35. White, I. M., Oveys, H. & Fan, X. Liquid core optical ring resonator sensors. *Opt. Lett.* **31,** 1319–1321 (2006).
36. Barrios, C. A. *et al.* Label-free optical biosensing with slot-waveguides. *Opt. Lett.* **33,** 708–710 (2008).
37. Bernardi, A. *et al.* On-chip Si/SiO_x microtube refractometer. *Appl. Phys. Lett.* **93,** 094106 (2008).
38. Li, H. & Fan, X. Characterization of sensing capability of optofluidic ring resonator biosensors. *Appl. Phys. Lett.* **97,** 011105 (2010).
39. Sumetsky, M., Dulashko, Y. & Windeler, R. S. Optical microbubble resonator. *Opt. Lett.* **35,** 898–900 (2010).
40. Testa, G., Huang, Y., Sarro, P. M., Zeni, L. & Bernini, R. Integrated silicon optofluidic ring resonator. *Appl. Phys. Lett.* **97,** 131110 (2010).
41. Grillet, C. *et al.* Compact tunable microfluidic interferometer. *Opt. Express* **12,** 5440–5447 (2004).
42. Song, W. Z. *et al.* Determination of single living cell's dry/water mass using optofluidic chip. *Appl. Phys. Lett.* **91,** 223902 (2007).
43. Song, W. Z. *et al.* Refractive index measurement of single living cells using on-chip Fabry–Pérot cavity. *Appl. Phys. Lett.* **89,** 203901 (2006).
44. Shao, H., Wang, W., Lana, S. E. & Lear, K. L. Optofluidic intracavity spectroscopy of canine lymphoma and lymphocytes. *IEEE Photon. Technol. Lett.* **20,** 493–495 (2008).
45. St-Gelais, R., Masson, J. & Peter, Y.A. All-silicon integrated Fabry–Pérot cavity for volume refractive index measurement in microfluidic systems. *Appl. Phys. Lett.* **94,** 243905 (2009).
46. Shumaker-Parry, J. S. & Campbell, C. T. Quantitative methods for spatially resolved adsorption/desorption measurements in real time by surface plasmon resonance microscopy. *Anal. Chem.* **76,** 907–917 (2004).
47. Ozkumur, E. *et al.* Label-free and dynamic detection of biomolecular interactions for high-throughput microarray applications. *Proc. Natl Sci. Acad. USA* **105,** 7988–7992 (2008).
48. Vollmer, F. *et al.* Protein detection by optical shift of a resonant microcavity. *Appl. Phys. Lett.* **80,** 4057–4059 (2002).
49. Zhu, H., White, I. H., Suter, J. D., Zourob, M. & Fan, X. Opto-fluidic micro-ring resonator for sensitive label-free viral detection. *Analyst* **133,** 356–360 (2008).
50. Ouyang, H., Striemer, C. C. & Fauchet, P. M. Quantitative analysis of the sensitivity of porous silicon optical biosensors. *Appl. Phys. Lett.* **88,** 163108 (2006).
51. Orosco, M. M., Pacholski, C. & Sailor, M. J. Real-time monitoring of enzyme activity in a mesoporous silicon double layer. *Nature Nanotechnol.* **4,** 255–258 (2009).
52. Manor, R. *et al.* Microfabrication and characterization of Teflon AF-coated liquid core waveguide channels in silicon. *IEEE Sens. J.* **3,** 687–692 (2003).
53. Cho, S. H., Godin, J. & Lo, Y.H. Optofluidic waveguides in Teflon AF-coated PDMS microfluidic channels. *IEEE Photon. Technol. Lett.* **21,** 1057–1059 (2009).
54. Korampally, V. *et al.* Development of a miniaturized liquid-core waveguide system with nanoporous dielectric cladding: A potential biosensing platform. *IEEE Sens. J.* **9,** 1711–1718 (2009).
55. Gopalakrishnan, N. *et al.* UV patterned nanoporous solid-liquid core waveguides. *Opt. Express* **18,** 12903–12908 (2010).
56. Fink, Y. *et al.* A dielectric omnidirectional reflector. *Science* **282,** 1679–1682 (1998).
57. Ganesh, N., Zhang, W., Mathias, P. C. & Cunningham, B. T. Enhanced fluorescence emission from quantum dots on a photonic crystal surface. *Nature Nanotechnol.* **2,** 515–520 (2007).
58. Smolka, S., Barth, M. & Benson, O. Highly efficient fluorescence sensing with hollow core photonic crystal fibers. *Opt. Express* **15,** 12783–12791 (2007).
59. Coscelli, E. *et al.* Toward a highly specific DNA biosensor: PNA-modified suspended-core photonic crystal fibers. *IEEE J. Sel. Top. Quant. Electron.* **16,** 967–972 (2010).
60. Liu, Y., Wang, S., Park, Y.S., Yin, X. & Zhang, X. Fluorescence enhancement by a two-dimensional dielectric annular Bragg resonant cavity. *Opt. Express* **18,** 25029–25034 (2010).
61. Xu, Q., Almeida, V. R., Panepucci, R. R. & Lipson, M. Experimental demonstration of guiding and confining light in nanometer-size lowrefractiveindex material. *Opt. Lett.***29,** 1626–1628 (2004).
62. Rudenko, M. I. *et al.* Ultrasensitive *Qβ* phage analysis using fluorescence correlation spectroscopy on an optofluidic chip. *Biosens. Bioelectron.* **24,** 3258–3263 (2009).
63. Chen, A. *et al.* Dual-color fluorescence cross-correlation spectroscopy on a planar optofluidic chip. *Lab Chip* **11,** 1502–1506 (2011).
64. Holmes, M. R. *et al.* Micropore and nanopore fabrication in hollow antiresonant reflecting optical waveguides. *J. Micro-Nanolith. MEM* **9,** 023004 (2010).
65. Kuhn, S. *et al.* Loss-based optical trap for on-chip particle analysis. *Lab Chip* **9,** 2212–2216 (2009).
66. Kuhn, S., Phillips, B. S., Lunt, E. J., Hawkins, A. R. & Schmidt, H. Ultralow power trapping and fluorescence detection of single particles on an optofluidic chip. *Lab Chip* **10,** 189–194 (2010).
67. Li, Z. & Psaltis, D. Optofluidic dye lasers. *Microfluid. Nanofluid.* **4,** 145–158 (2007).

68. Moskovits, M. Surface roughness and the enhanced intensity of Raman scattering by molecules adsorbed on metals. *J. Chem. Phys.* **69,** 4159–4161 (1978).
69. Michaels, A. M., Nirmal, M. & Brus, L. E. Surface enhanced Raman spectroscopy of individual rhodamine 6G molecules on large Ag nanocrystals. *J. Am. Chem. Soc.* **121,** 9932–9939 (1999).
70. Saikin, S. K., Chu, Y., Rappoport, D., Crozier, K. B. & Aspuru-Guzik, A. Separation of electromagnetic and chemical contributions to surface-enhanced Raman spectra on nanoengineered plasmonic substrates. *J. Phys. Chem. Lett.* **1,** 2740–2746 (2010).
71. Nie, S. & Emory, S. R. Probing single molecules and single nanoparticles by surface-enhanced Raman scattering. *Science* **275,** 1102–1106 (1997).
72. Kneipp, K. *et al.* Single molecule detection using surface-enhanced Raman scattering (SERS). *Phys. Rev. Lett.* **78,** 1667–1670 (1997).
73. Jeanmaire, D. L. & Duyne, R. P. V. Surface Raman spectroelectrochemistry part I: Heterocyclic, aromatic, and aliphatic amines adsorbed on the anodized silver electrode. *J. Electroanal. Chem.* **84,** 1–20 (1977).
74. Albrecht, M. G. & Creighton, J. A. Anomalously intense Raman spectra of pyridine at a silver electrode. *J. Am. Chem. Soc.* **99,** 5215–5217 (1977).
75. Yang, X. *et al.* High-sensitivity molecular sensing using hollow-core photonic crystal fiber and surface-enhanced Raman scattering. *J. Opt. A* **27,** 977–985 (2010).
76. Khaing Oo, M. K., Han, Y., Kanka, J., Sukhishvili, S. & Du, H. Structure fits the purpose: Photonic crystal fibers for evanescent-field surface-enhanced Raman spectroscopy. *Opt. Lett.* **35,** 466–469 (2010).
77. Measor, P. *et al.* On-chip surface-enhanced Raman scattering detection using integrated liquid-core waveguides. *Appl. Phys. Lett.* **90,** 211107 (2007).
78. Wang, M., Jing, N., Chou, I.H., Cote, G. L. & Kameoka, J. An optofluidic device for surface enhanced Raman spectroscopy. *Lab Chip* **7,** 630–632 (2007).
79. Park, S.M., Huh, Y. S., Craighead, H. G. & Erickson, D. A method for nanofluidic device prototyping using elastomeric collapse. *Proc. Natl Sci. Acad. USA* **106,** 15549–15554 (2009).
80. Liu, J., White, I. & DeVoe, D. L. Nanoparticle-functionalized porous polymer monolith detection elements for surface-enhanced Raman scattering. *Anal. Chem.* **83,** 2119–2124 (2011).
81. Huh, Y. S., Chung, A. J., Cordovez, B. & Erickson, D. Enhanced on-chip SERS based biomolecular detection using electrokinetically active microwells. *Lab Chip* **9,** 433–439 (2009).
82. Cho, H., Lee, B., Liu, G. L., Agarwal, A. & Lee, L. P. Label-free and highly sensitive biomolecular detection using SERS and electrokinetic preconcentration. *Lab Chip* **9,** 3360–3363 (2009).
83. White, I. M., Gohring, J. & Fan, X. SERS-based detection in an optofluidic ring resonator platform. *Opt. Express* **15,** 17433–17442 (2007).
84. Kim, S.-M., Zhang, W. & Cunningham, B. T. Photonic crystals with SiO_2–Ag 'post-cap' nanostructure coatings for surface enhanced Raman spectroscopy. *Appl. Phys. Lett.* **93,** 143112 (2008).
85. Choi, I., Huh, Y. S. & Erickson, D. Size-selective concentration and label-free characterization of protein aggregates using a Raman active nanofluidic device. *Lab Chip* **11,** 632–638 (2011).
86. Walter, A., Marz, A., Schumacher, W., Rosch, P. & Popp, J. Towards a fast, high specific and reliable discrimination of bacteria on strain level by means of SERS in a microfluidic device. *Lab Chip* **11,** 1013–1021 (2011).
87. Eriksson, E. *et al.* Optical manipulation and microfluidics for studies of single cell dynamics. *J. Opt. A* **9,** S113–S121 (2007).
88. Wang, T.H., Peng, Y., Zhang, C., Wong, P. K. & Ho, C.M. Single-molecule tracing on a fluidic microchip for quantitative detection of low-abundance nucleic acids. *J. Am. Chem. Soc.* **127,** 5354–5359 (2005).
89. Wang, K., Schonbrun, E., Steinvurzel, P. & Crozier, K. B. Scannable plasmonic trapping using a gold stripe. *Nano Lett.* **10,** 3506–3511 (2010).
90. Mandal, S. & Erickson, D. Nanoscale optofluidic sensor arrays. *Opt. Express* **16,** 1623–1631 (2008).
91. Arnold, S. *et al.* Whispering gallery mode carousel: A photonic mechanism for enhanced nanoparticle detection in biosensing. *Opt. Express* **17,** 6230–6238 (2009).
92. Lin, S., Schonbrun, E. & Crozier, K. Optical manipulation with planar silicon microring resonators. *Nano Lett.* **10,** 2408–2411 (2010).
93. Applegate, R. W., Squier, J., Vestad, T., Oakey, J. & Marr, D. W. M. Optical trapping, manipulation, and sorting of cells and colloids in microfluidic systems with diode laser bars. *Opt. Express* **12,** 4390–4398 (2004).
94. Chiou, P. Y., Ohta, A. T. & Wu, M. C. Massively parallel manipulation of single cells and microparticles using optical images. *Nature* **436,** 370–372 (2005).
95. Cui, X. *et al.* Lensless high-resolution on-chip optofluidic microscopes for *Caenorhabditis elegans* and cell imaging. *Proc. Natl Sci. Acad. USA* **105,** 10670–10675 (2008).
96. Bishara, W., Su, T.W., Coskun, A. F. & Ozcan, A. Lensfree on-chip microscopy over a wide fieldofview using pixel super-resolution. *Opt. Express* **18,** 11182–11191 (2010).
97. Villatoro, J. *et al.* Photonic crystal fiber interferometer for chemical vapor detection with high sensitivity. *Opt. Express* **17,** 1447–1453 (2009).
98. Cubillas, A. M. *et al.* Methane detection at 1670-nm band using a hollow-core photonic bandgap fiber and a multiline algorithm. *Opt. Express* **15,** 17570–17576 (2007).
99. Zhao, B. S., Koo, Y.M. & Chung, D. S. Separations based on the mechanical forces of light. *Anal. Chim. Acta* **556,** 97–103 (2006).

Acknowledgements

The authors acknowledge support from the National Science Foundation (ECCS-1045621 and CBET-1037097) and the National Institute of Biomedical Imaging and Bioengineering (5K25EB006011).